NUCET NUCLEAR ENERGY AND TECHNOLOGY

Nuclear Energy and Technology 5(4): 361–371
DOI 10.3897/nucet.5.39096

Research Article

Different distributions of gold nanoparticles on the tumor and calculation of dose enhancement factor by Monte Carlo simulation

Sajad Keshavarz[1], Dariush Sardari[1]

1 *Department of Medical Radiation Engineering, Science and Research Branch, Islamic Azad University, Tehran, Iran*

Corresponding author: *Sajad Keshavarz* (sajadkeshavarz7@gmail.com)

Academic editor: *Boris Balakin* ♦ **Received** 17 August 2019 ♦ **Accepted** 28 October 2019 ♦ **Published** 10 December 2019

Citation: Keshavarz S, Sardari D (2019) Different distributions of gold nanoparticles on the tumor and calculation of dose enhancement factor by Monte Carlo simulation. Nuclear Energy and Technology 5(4): 361–371. https://doi.org/10.3897/nucet.5.39096

Abstract

Gold nanoparticles can be used to increase the dose of the tumor due to its high atomic number as well as being free from apparent toxicity. The aim of this study is to evaluate the effect of distribution of gold nanoparticles models, as well as changes in nanoparticle sizes and spectrum of radiation energy along with the effects of nanoparticle penetration into surrounding tissues in dose enhancement factor DEF. Three mathematical models were considered for distribution of gold nanoparticles in the tumor, such as 1-uniform, 2- non-uniform distribution with no penetration margin and 3- non-uniform distribution with penetration margin of 2.7 mm of gold nanoparticles. For this purpose, a cube-shaped water phantom of 50 cm size in each side and a cube with 1 cm side placed at depth of 2 cm below the upper surface of the cubic phantom as the tumor was defined, and then 3 models of nanoparticle distribution were modeled. MCNPX code was used to simulate 3 distribution models. DEF was evaluated for sizes of 20, 25, 30, 50, 70, 90 and 100 nm of gold nanoparticles, and 50, 95, 250 keV and 4 MeV photon energies. In uniform distribution model the maximum DEF was observed at 100 nm and 50 keV being equal to 2.90, in non-uniform distribution with no penetration margin, the maximum DEF was measured at 100 nm and 50 keV being 1.69, and in non-uniform distribution with penetration margin of 2.7 mm, the maximum DEF was measured at 100 nm and 50 keV as 1.38, and the results have been showed that the dose was increased by injecting nanoparticles into the tumor. It is concluded that the highest DEF could be achieved in low energy photons and larger sizes of nanoparticles. Non-uniform distribution of gold nanoparticles can increase the dose and also decrease the DEF in comparison with the uniform distribution. The non-uniform distribution of nanoparticles with penetration margin showed a lower DEF than the non-uniform distribution without any margin and uniform distribution. Meanwhile, utilization of the real X-ray spectrum brought about a smaller DEF in comparison to mono-energetic X-ray photons.

Keywords

dose enhancement, gold nanoparticles, distribution, nanoparticle size, Monte Carlo

1. Introduction

Cancer is one of the main reasons of fatality and one of the treatment methods for curing this ailment can be radiotherapy. The main purpose in radiotherapy is to give lethal dose to the tumor and protecting the normal tissues. One of the methods we can implement here is the use of nanoparticle in treatment and diagnosis. Nanoparticles can enhance the efficiency of diagnosis and treatment of cancer. The purpose of new radiation therapy techniques

is reducing the absorbed dose in healthy tissues (Mousavie Anijdan et al. 2008). Since the major interaction of photons inside the tumor depends on the photon energy and target atomic number, gold with Z=79 is a proper candidate to be formed as nanoparticles and can enter into a tumor. Gold nanoparticles (GNPs) have longer retention time in a tumor. Therefore, they can be attached to the tumor (Cho 2005, Rahman et al. 2009). Another property which makes gold favorable is its non-toxicity to human (Alkilany and Murphy 2010). The positive effect of high-Z elements in radiation dose enhancement dates back to the 1970's (Granqvist et al. 1976, Hayashi et al. 1997) in the Exploratory Research for Advanced Technology (ERATO) research program.

The effect of iodine concentration and radiation quality on growing lymphocytes as well as the effect of the dose after injection of iodine in the brain of rabbits was reviewed by Mello et al. (1983). It was also observed that direct injection of iodine into the tumor with the x-ray of 100 keV stopped about 80% of tumor growth completely. Other elements such as platinum (Kobayashi et al. 2003, Adam et al. 2008), gadolinium (Prezado et al. 2009) and gold (Cho 2005, Mello et al. 1983, Hainfeld et al. 2004, Chang et al. 2008, Herold et al. 2000, Roeske et al. 2007, Zheng et al. 2008, Brun et al. 2009) have been put into practice. Herold et al. (2000) injected gold microparticles with 1.5–3 microns diameter into tumor cells of mice directly and used radiations with energy spectrum of 100, 140, 200 and 240 keV X-ray and Cs-137 brachytherapy source. They measured cell survival cologenic method and increased the dose in the mentioned energies. Robert et al. (2009) studied the dose enhancement factor of iodine and gadolinium in tumor irradiated with x-ray spectrum of a medical linac. Intravenous injection of nanoparticles with 1.9 nm dimensions and 2.7 mg⁄ml of concentration in tumoral cells of mouse in 250 keV was performed by Hainfeldet al. (2004) and cell survival was measured. Cell survival, a combination of gold nanoparticle with x-ray was 86% versus 20% with x-ray alone and 0% gold alone. Besides, the same research group has shown, in 2008 (Hainfeld et al. 2008), that radiation therapy along with an intervascular injection of gold nanoparticles in a mouse model leads to complete shrinkage of tumor in 86% of cases. The effect of nanoparticles in radiation therapy with 140keV, 4 MeV, 6MeV x-ray and with gamma photons of the 192Ir source was studied using Monte Carlo (MC) method by Cho (2005). The effect of gold nanoparticles on dose enhancement with 192Ir source photons was simulated with Geometry and Tracking (GEANT4) code by Zhang et al. (2009). Lin et al. (2014) have compared the case of kilovoltage and megavoltage photons and proton for dose enhancement and exhibited that the proton dose can be increased up to 14 times, and this does not depend on proton energy, while the photon dose depends upon the photon energy.

Energy optimization in gold nanoparticle enhanced radiation therapy by Monte Carlo simulation in the brain and breast tumors in kilovoltage and orthovoltage beam energy has been compared by Sung et al. (2018). they showed for breast using a single photon beam, kilovoltage with Gold NanoParticle (kV+GNP) was found to yield up to 2.73 times higher mean relative biological effectiveness (RBE)-weighted dose to the tumor than two tangential MegaVoltage (MV) beams while delivering the same dose to healthy tissue and for irradiation of brain tumors using multiple photon beams, the GNP dose enhancement was found to be effective for energies above 50 keV.

Local Effect Model (LEM)-based predictions of radio-enhancement were suggested based on the ideas of heterogeneous dose distributions inside the cell in GNP-enhanced x-ray therapy (Sung et al. 2017).

Size-dependent tissue kinetics of Polyethylene Glycol (PEG)-coated gold nanoparticles was studied by Cho et al. (2010). They performed a kinetic study in mice with different sizes of PEG-coated Au-Nano particles (AuNPs). Small AuNPs (4 and 13 nm) showed high levels of concentration in the blood for 24 h and were cleared by 7 days, whereas large (100 nm) AuNPs were completely cleared by 24 h. Small AuNPs transiently activated CYP1A1 and 2B metabolic enzymes, in liver tissues from 24 h to 7 days, which mirrored with elevated gold levels in the liver. Large AuNPs did not affect metabolic enzymes.

Sakata et al. (2018) compared microscopic and macroscopic doses with Geant4-DNA track-structure simulation. They wrote a simulation program to calculate the absorbed dose in liquid water around the gold nanoparticles. The new physics models show similar backscattering coefficients with the existing Geant4 Livermore and Penelope models in large volumes for 100 keV incident electrons.

In previous studies, commonly iodine and gadolinium were used, but in this study, instead of iodine and gadolinium, gold nanoparticles due to their high atomic number, inaction, and better bio-compatibility are used. The formation of more surface bonds between biomolecules and gold nanoparticles and ~3-times more photon absorption than iodine at 20 and 100 keV energy (Hainfeld et al. 2008) makes GNP an excellent candidate for radiation therapy purposes. The effect of radiation quality and contrast concentration in uniform distribution of nanoparticles in tumor was studied (Mesbahi et al. 2013), but in the present study, the effect of radiation energy and the size of gold nanoparticles as well as the effect of penetration margin of nanoparticles in healthy tissues were investigated in three models: 1-uniform distribution, 2- non-uniform distribution with no penetration margin, 3 non-uniform distribution with 2.7 mm penetration margin.

2. Materials and methods

2.1. Description of the geometry of tumor and phantom

As it is illustrated in Fig. 1, a cube – shaped water phantom of 50 cm size in each side was simulated with Monte Carlo N-particle transport code system (MCNP) code (Mesbahi et al. 2013, MCNP 1997). The geometric cen-

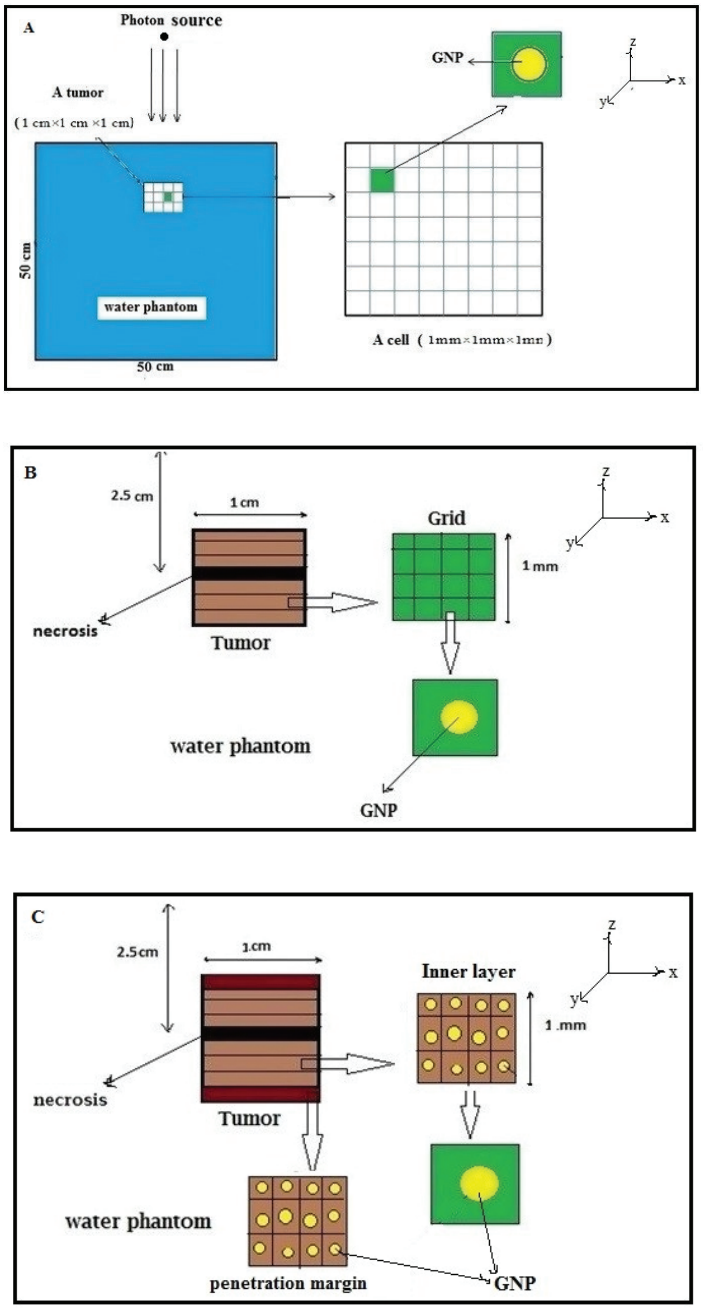

Figure 1. Location of tumor in phantom and the mesh size for computation. (A): uniform distribution of GNPs, (B): Non-uniform distribution of GNPs while the central layer is in the necrosis state. Each layer of thickness 1 mm is divided into sublayers, (C): Non-uniform distribution of GNPs with penetration margin of 2.7 mm for the tumor.

ter of the cube was $X=Y=Z=0$. The tumor was defined as a cube with 1 cm side located at 2 cm depth below the upper surface of the cubic phantom which was composed of soft tissue (Harry et al. 1989). The photon point source was 100 cm above the phantom surface in the Z direction. Inside the cubic tumor, 18 mg gold nanoparticles per 1 g tissue were dissolved while the mass density of gold was 19.32 g/cm^3 and the tumor volume was divided to a mesh with lattice card in the code. In non-uniform distribution of GNP, tumor was divided into 11 layers. Based on the concentration and density of gold nanoparticles, different distributions for nanoparticles in the tumor were considered and the dose was calculated with F6 and *F8 tally cards. Tally cards are used to specify what type of information the user wants to gain from the Monte Carlo calculation. F6 tally is used to calculate Energy deposition averaged over a cell and *F8 tally is used to calculated energy deposition tally too. then according to equation (2) the dose enhancement factor (DEF) was calculated. In this study History Cutoff (NPS) was 1×10^9. NPS is the number of histories of a particle that has been tracked.

2.2. Modeling and simulation of gold nanoparticles distribution in tumor

Three kinds of spatial distributions were considered for gold nanoparticles inside the tumor as below:

- Uniform distribution
- Non-uniform distribution without any penetration margin
- Non-uniform distribution with a margin for nanoparticles for penetration into healthy tissue.

2.2.1. Uniform distribution

This is the most ideal case for distribution of nanoparticles. In this model, it was assumed that nanoparticles were uniformly distributed all over the tumor volume and there were no nanoparticles outside the tumor and therefore:

$$C(r)=\begin{cases} C & \text{if } 0\le r\le A \\ 0 & \text{if } r>A \end{cases} \quad (1)$$

In this equation, A is the side of the cube and r is the distance of an arbitrary point from the tumor center. C is the concentration of gold nanoparticles.

As it was mentioned before, in Fig. 1A, the tumor was modeled as a 1 × 1 × 1 cm cube in 2 cm depth. With lattice card in MCNP code, this volume were divided into 1 mm×1mm×1mm smaller cubes and the source was simulated as a point source. In each of such cubes, enough numbers of gold nanoparticles was defined according to the concentration of 18 mg/cm^3 and sizes of 20, 25, 30, 50, 70, 90 and 100 nm of GNPs (Mesbahi et al. 2013). With the use of F6 tally and assuming the equality between dose and kerma, the average dose in the 1mm^3 voxel was computed with and without the presence of GNPs in the Z direction. Then the DEF was obtained by equation (2).

$$\text{DEF}=\frac{\text{Averge dose with GNPs}}{\text{Aveage dose without GNPs}} \quad (2)$$

In this study, such computations were carried out for x-ray spectra generated by 50, 95, 250 keV and 4 MV linear accelerators (Sheikh-Bagheri and Rogers 2002). Besides, monoenergetic photons of 50, 95, and 250 keV were considered. The calculation error was less than 3%, which was calculated by simulation software MCNP.

2.2.2. Non-uniform model without penetration margin

As a matter of fact, the blood circulation in the tumor surface is much more than its internal layers and the tumor core is normally a necrosis volume. Therefore, it is expected to exist less concentration of nanoparticles as it is deeper into the tumor. The cubical tumor was divided into 11 layers for showing the change of absorption gold nanoparticle form surface of tumor to the center of the tumor that it was assumed 1 layer was in the center of the tumor (necrosis) and 5 layers were upper than the necrosis layer and 5 layers were below the necrosis layer. Such distribution of nanoparticles is described by $C_i = a.exp(z)-k$. Which C_i is the amount of concentration in each layer and a is a constant number that depends on the total concentration, and k is a constant number and z is the distance from the center of the tumor. In the present work, the cubical tumor shape was divided into 11 shells (layers) with different concentrations that reduced as the shell was closer to the center of the tumor. Till in the central layer the concentration becomes zero ($C_i = 0$).With considering $C_i = 0$ in $C_i = a.exp(z)-k$, it obtained:

$$\begin{cases} C_i = 0 \\ z = 0 \end{cases} \rightarrow C_i = ae^z - k \rightarrow 0 = ae^0 - k \rightarrow a = k$$
$$C_i = a\left(e^z - 1\right) \quad (3)$$

Considering the above relation and that the integral of this equation (3) is equal to the total concentration of nanoparticles on the tumor from the center ($z = 0$) to the surface of the tumor ($z = 0.5$ cm), and total concentration of nanoparticle in this study is $C_T = 18$ mg/ml and then the value of a and k are calculated:

$$\int_0^{0.5} C_i dz = C_T$$
$$\int_0^{0.5} C_i dz = \int_0^{0.5} a\left(e^z - 1\right)dz = C_T$$
$$a\left(e^{0.5} - 1.5\right) = 18$$
$$a = k = 0.121$$

Therefore, the distribution of nanoparticle in each layer in the tumor is obtained:

$$C_i = 0.121\exp(z) - 0.121 \quad (4)$$

As it can be observed in Fig. 1B, the computational procedure was carried out in 11 regions inside the tumor. Nanoparticle concentration was estimated by equation (4) in each layer. Then in MCNP code, each region might be subdivided into small cubes using “lattice card” and in each cube, one nanoparticle was placed. The value of radiation dose in each layer was obtained and the DEF in every layer for the tumor was computed. *F8 tally was considered for computation of absorbed dose. *F8 is an energy deposition tally, which is used to calculate the energy deposited in each computational cell, and its unit is MeV, which should be divided per mass of that cell to calculate the dose. In this model, no nanoparticle is penetrated into the healthy tissue. With the use of the non-penetration model, DEF was computed for X-rays of 50, 95 and 250 keV energy and for X-ray generated with 4MV Varian linac with the same size of nanoparticles as it was mentioned before.

2.2.3. Non-uniform model with penetration margin

In clinical practice, it was observed that deposition of nanoparticles is not restricted to only tumor volume (Cho 2005). In other words, in clinical application due to different angiogenesis and lack of blood supply to all parts of the tumor, gold nanoparticles are not uniformly distributed through the tumor volume. A number of nanoparticles

penetrate into the surrounding tissues and cause a decrease of nanoparticle concentration inside the tumor. This effect was considered by developing a margin of 2.7mm thickness around the tumor in which nanoparticle concentration was 5 mg/cm^3 (the ratio of gold nanoparticle concentration inside the tumor to outside of the tumor is 3.5:1) as it is described in Fig. 1C). The rest of the computational method was similar to that which was described for the previous model, and the concentration of nanoparticles inside the penetration margin is equal to 5 mg/cm^3 and the concentration of gold in the tumor 13 mg/cm^3. So:

$$C_i = a\left(e^z - 1\right)$$

$$\int_0^{0.5} C_i dz = C_T$$

$$\int_0^{0.5} C_i dz = \int_0^{0.5} a\left(e^z - 1\right) dz = C_T$$

$$a\left(e^{0.5} - 1.5\right) = 13$$

$$a = k = 0.0087$$

Therefore, the distribution of nanoparticle in each layer in the tumor is obtained:

$$C_i = 0.0087e^z - 0.0087 \qquad (5)$$

In this equation, C_i is the amount of concentration in each layer and z is the distance from the center of the tumor.

The calculation an uncertainty was less than 3%. DEF has been computed for X-rays of 50, 95, 250 keV and for X-ray generated with 4MV with Varian linac with the same size of nanoparticles. It is noteworthy that the DEF was also obtained for some points outside the tumor in the z-direction.

3. Results

3.1 DEF in the uniform model

The results of DEF with different sizes of gold nanoparticles (20, 25, 50, 70, 90 and 100 nm) in 50, 95, 250 keV and 4 MeV energies with 18 mg/cm^3 concentration in the uniform distribution are revealed in Fig. 2A–D, respectively. Additionally, the average dose enhancement factor (DEF) over the whole tumor volume of 1 cm × 1 cm × 1 cm cube for different photon energies and GNP sizes in the uniform model is listed in Table 1.

Variation of dose enhancement factor based on the size of nanoparticles and energy of X-rays in the uniform model is demonstrated in Figs 3, 4, respectively.

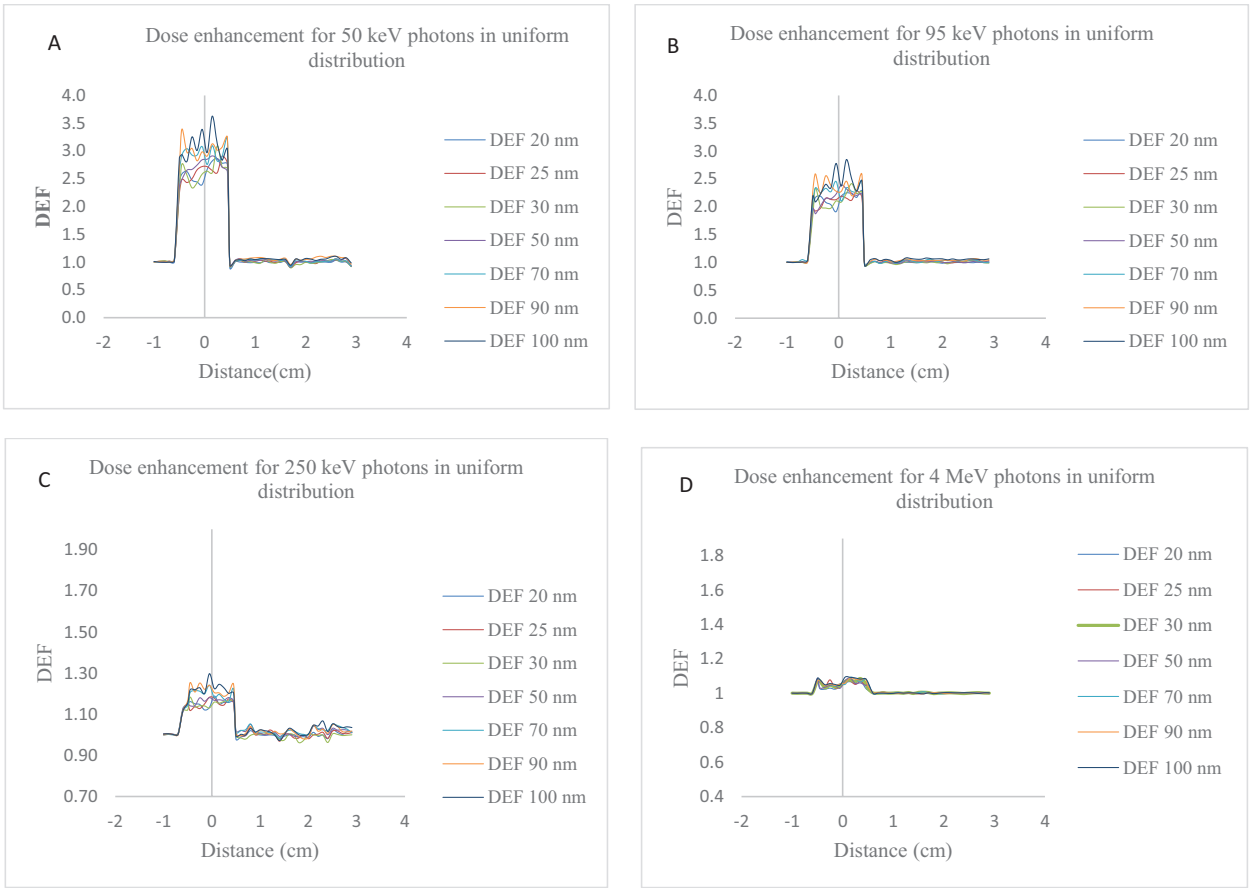

Figure 2. Dose enhancement in tumor and surrounding tissues according to a uniform model for different sizes of GNPs. The photon energy is 50, 95, 250 keV and 4 MV from a linac, (A), (B), (C), (D) respectively.

Table 1. Average dose enhancement factor (DEF) in the whole volume for different photon energies and GNP sizes for the uniform model.

	Diameter of GNPs						
	20 nm	25 nm	30 nm	50 nm	70 nm	90 nm	100 nm
50 keV	2.46	2.47	2.48	2.55	2.76	2.85	2.90
95 keV	2.01	2.02	2.03	2.06	2.18	2.25	2.28
250 keV	1.13	1.13	1.14	1.15	1.18	1.19	1.20
4 MV	1.04	1.05	1.05	1.05	1.06	1.06	1.07

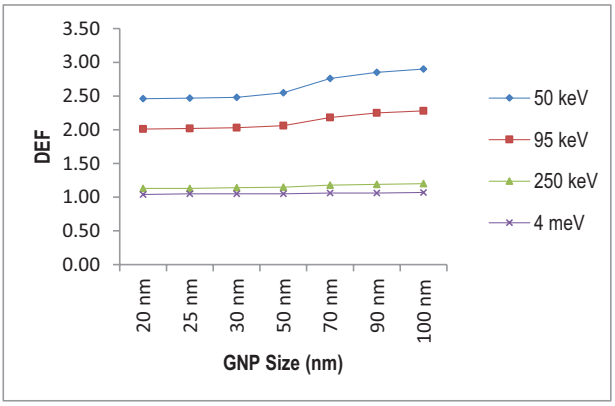

Figrue 3. Variation of dose enhancement factor with a size of nanoparticles in the uniform model.

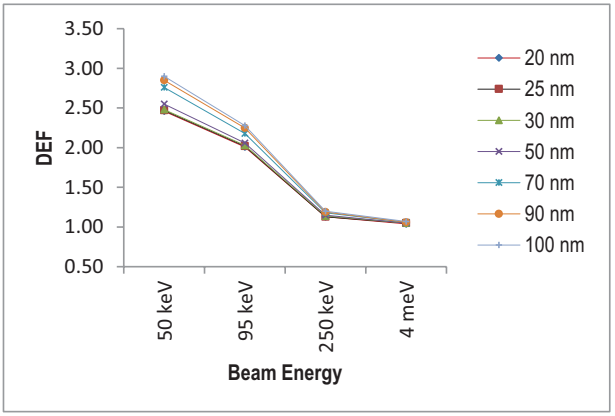

Figrue 4. Variation of dose enhancement factor with X-ray energy in the uniform model.

3.2 DEF in the non-uniform model without penetration margin

The results of DEF with variation of the size of gold nanoparticles (20, 25, 50, 70, 90 and 100 nm) in 50, 95, 250 keV and 4 MV energies in the 18 mg/cm^3 of concentration in the uniform distribution without penetration margin are displayed in Fig. 5A–D), respectively. Furthermore, the average dose enhancement factor (DEF) over the whole tumor volume of 1 cm × 1 cm × 1 cm cube for different photon energies and GNP sizes in the uniform model without penetration margin is elaborated in Table 2.

Variation of dose enhancement factor versus the size of nanoparticles and energy of X-rays in the uniform model without penetration margin is presented in Fig. 6 and Fig. 7, respectively.

Table 2. Average dose enhancement factor (DEF) in the whole volume for different photon energies and GNP sizes for the non-uniform model.

	Diameter of GNPs						
	20 nm	25 nm	30 nm	50 nm	70 nm	90 nm	100 nm
50 keV	1.49	1.51	1.52	1.54	1.60	1.65	1.69
95 keV	1.23	1.23	1.26	1.27	1.29	1.31	1.33
250 keV	1.06	1.07	1.08	1.08	1.08	1.09	1.09
4 MV	1.04	1.05	1.05	1.06	1.07	1.07	1.08

3.3 DEF in a non-uniform model with penetration margin

The results of DEF with variation of the size of gold nanoparticles (20, 25, 50, 70, 90 and 100 nm) in 50, 95, 250 keV and 4 MV energies with 18 mg/cm^3 concentration in the uniform distribution with 2.7 mm penetration margin are depicted in Fig. 8A–D, separately. Moreover, the average dose enhancement factor (DEF) over the whole tumor volume of 1 cm × 1 cm × 1 cm cube for different photon energies and GNP sizes in the uniform model with a 2.7 mm penetration margin is portraited in Table 3.

Variation of dose enhancement factor with the size of nanoparticles and energy of X-raysin the uniform model with a 2.7 mm penetration margin is shown in Figs 9, 10, respectively.

4. Discussion

In this study, the effect of uniform and non-uniform distribution of gold nanoparticles in the tumor, the effect of nanoparticle sizes, the effect of energy on the tumor dose enhancement and the effect of the margin of penetration of gold nanoparticles into healthy tissues around the tumor were taken into consideration.

Dose enhancement factor was calculated in three models of uniform distribution, non-uniform distribution with no penetration margin and non-uniform distribution with a margin of 2.7 mm penetration of gold nanoparticles to surrounding healthy tissue. Figrue 2A–D indicates that the absorbed dose is increased in the presence of nanoparticles. In this figure, dose enhancement was drawn versus the depth of the tumor in the direction of the radiation beam. In Table 1 DEF is calculated with equation (6). According to Fig. 2A–D and Table 1, DEF is more pronounced in lower energies than in higher energies. Additionally, the larger diameter of nanoparticles provides more DEF than the smaller diameter. This is better seen in Fig. 3 in which DEF was drawn versus GNP size. And it is observed that above the energy of 250 keV, the DEF would be very close to 1.0, and this means that the presence of GNP has almost no effect. As it is understood from Fig. 4, in the uniform distribution model, the DEF is remarkable for a photon of energies below 100 keV. The highest DEF exists for GNP diameter of 100 nm and photon energy of 50 keV which amounts to 2.90. These results are consistent with the results of Mesbahi et al about the effect of Photon Beam Energy, GNPs Size and

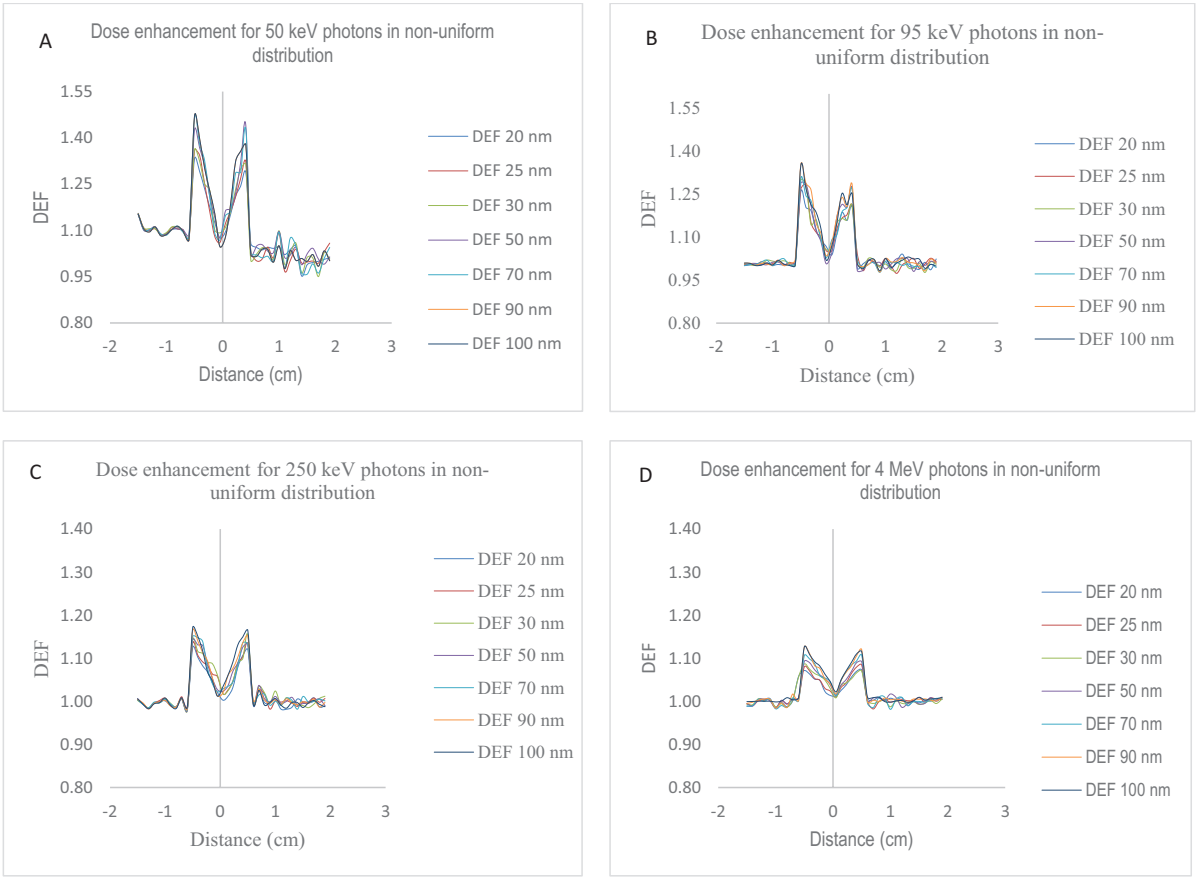

Figure 5. Dose enhancement in tumor and surrounding tissues according to a non-uniform model without penetration margin for different sizes of GNPs. The photon energy is 50, 95, 250 keV and 4 MV linac, (A), (B), (C), (D) respectively.

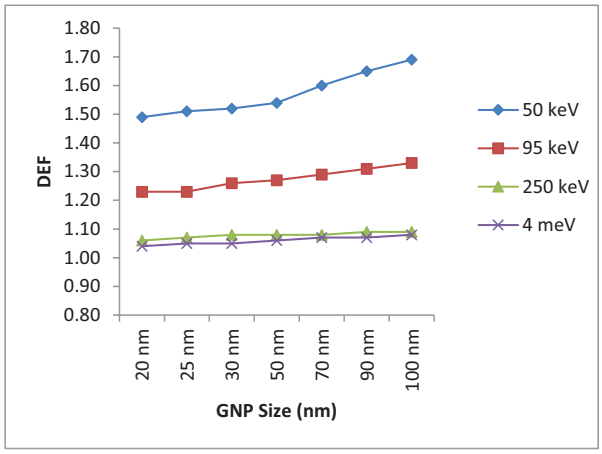

Figure 6. Variation of dose enhancement factor with X-ray energy in the non-uniform model without penetration margin.

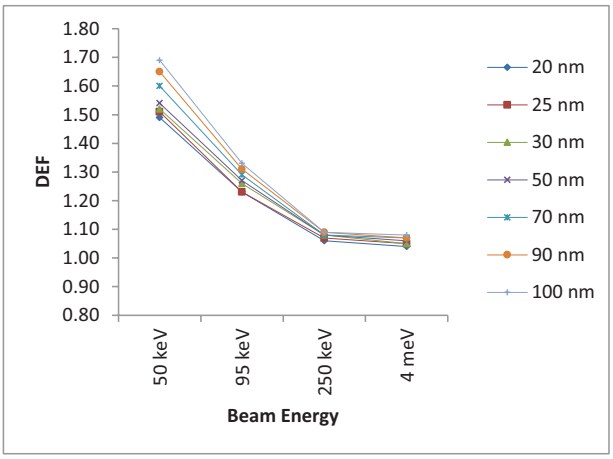

Figure 7. Variation of dose enhancement factor with X-ray energy in the non-uniform model without penetration margin.

concentration on the dose enhancement in radiation therapy (Mesbahi et al. 2013).

The results of DEF computations for the non-uniform distribution are shown in Fig. 5A–D). In this case, in the central part of the tumor due to necrosis, no dose enhancement is observed, especially when the part of the tumor closer to the surface is on the focus of attention. This is the evidence of the dependence of DEF on GNP concentration. According to this figure and the data in Table 2, it is understood that in a general view the DEF in the non-uniform model is less than that of the uniform model. In the non-uniform distribution of GNPs, the surface of the tumor has the highest absorbed dose and the center of the tumor has the lowest absorbed dose due to the necrosis.

According to Fig. 7 the DEF increases with photon energy up to a maximum value that happens close to 95

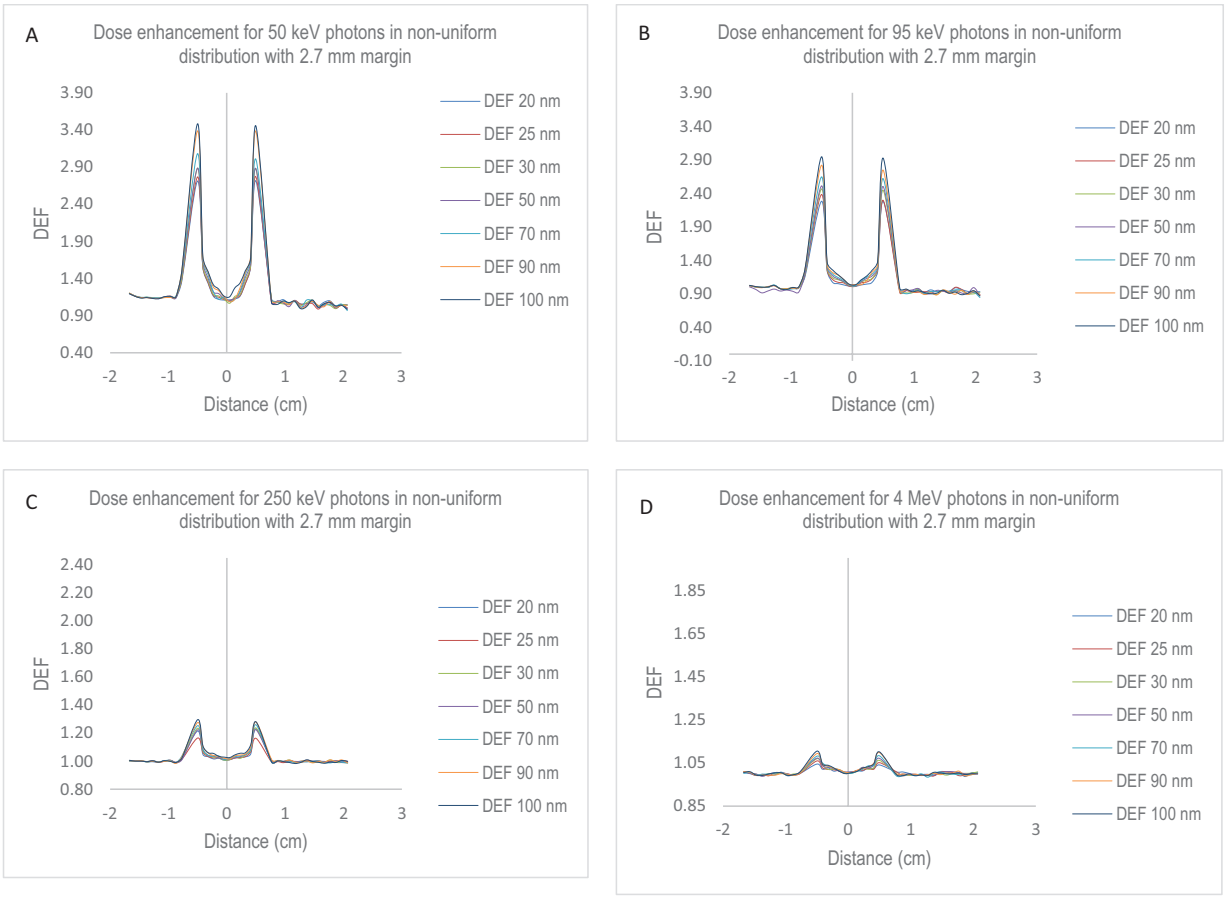

Figure 8. Dose enhancement in tumor and surrounding tissues according to a non-uniform model with 2.7 mm penetration margin for different sizes of GNPs. The photon energy is 50, 95, 250 keV and 4 MV, (A), (B), (C), (D), respectively.

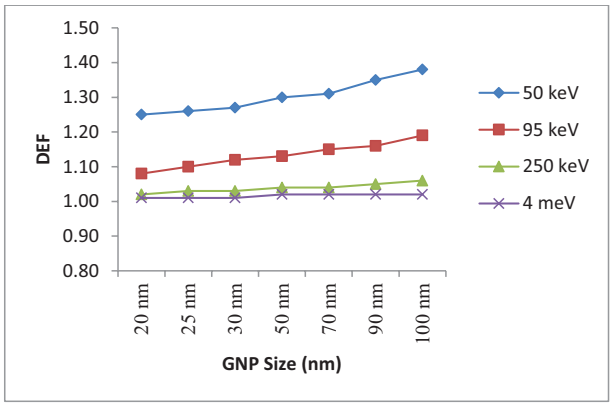

Figure 9. Variation of dose enhancement factor with the size of nanoparticles for the non-uniform model with a 2.7 mm penetration margin.

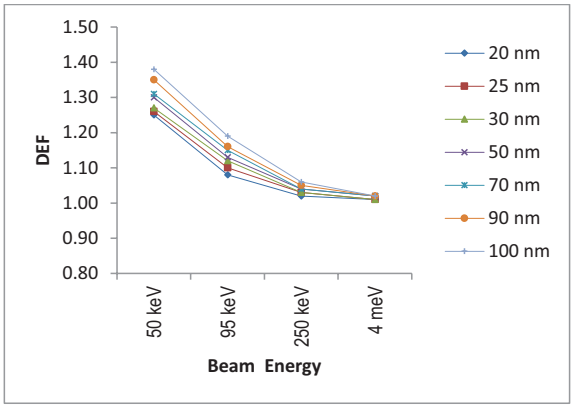

Figure 10. Variation of dose enhancement factor with X-ray energy for the non-uniform model with a 2.7 mm penetration margin.

Table 3. Average dose enhancement factor (DEF) in the whole volume for various photon energies and GNP sizes for the non-uniform model with a 2.7 mm penetration margin.

	Diameter of GNPs						
	20 nm	25 nm	30 nm	50 nm	70 nm	90 nm	100 nm
50 keV	1.25	1.26	1.27	1.30	1.31	1.35	1.38
95 keV	1.08	1.10	1.12	1.13	1.15	1.16	1.19
250 keV	1.02	1.03	1.03	1.04	1.04	1.05	1.06
4 MV	1.01	1.01	1.01	1.02	1.02	1.02	1.02

keV, which is due to K-edge of gold. Therefore, the optimum energy for DEF in non-uniform distribution without penetration margin is 50 keV with GNP of 100 nm with DEF amounting to 1.69.

In the non-uniform model with a 2.7 mm penetration margin, 5 mg/cm^3 of 18 mg/cm^3 of gold concentration penetrates to the healthy tissue. This leads to lower DEF in comparison with two cases of uniform and non-uniform distributions in the tumor. This phenomenon is shown in

Fig. 8A–D. The numerical data for this case are listed in Table 3. As it was observed before, in this case, the highest DEF happens for 100 nm of nanoparticle dimensions. In this model, as well as in the other previously studied models, the highest DEF observed in the lowest photon energy. The highest DEF is encountered for GNP size of 100 nm at a photon energy of 50 keV which is equal to 1.38.

In other words, In the uniform distribution, the maximum DEF of 2.90 occurs for 100 nm diameter of gold nanoparticles and 50 keV X-ray energy. In the non-uniform model which lacks the margin case, DEF of 1.69 happens for 100 nm nanoparticles and 50 keV X-ray. When a penetration margin is considered for nanoparticles, DEF of 1.38 happens for 100 nm nanoparticles and 50 keV X-rays. Additionally, in the non-uniform distribution of gold nanoparticles, has been used for two distribution models: 1. Non-uniform distribution without penetration margin. 2. Non-uniform distribution with a margin of 2.7 mm penetration of gold nanoparticles to surrounding tissues. It has been clarified that the DEF in the non-uniform model with the penetration margin is less than DEF in the non-uniform model without margin.

In a study by Cho (2005) a concentration of 2 mg/g was considered in normal tissue and this resulted in a negligible dose enhancement in the normal tissues around the tumor. In the present work, the introduction of gold nanoparticles in the penetration of margin of the tumor was not performed and this effect can be a subject of further research in this field. Ranjbar, et al. (2010) have revealed that with 10 mgAu/ml homogeneous GNPs in 85 keV photon energy for the case of a tumor located at 4.5 cm depth, DEF is 1.80 and decreases with increasing depth.

In another study, in Computational Fluid Daynamics (CFD) model, the effect of the size of magnetic nanoparticles on the energy absorption in solar collector has been investigated. By increasing the nanoparticle size to about 100 nm, thermal efficiency has been increased, but larger than 100 nm, the thermal efficiency has been reduced (Guo et al. 2017, Balakin et al. 2019). Similar behavior in the present study was observed for GNP size less than 100 nm meaning that the dose enhancement factor has been increased with increasing size of the gold nanoparticles.

Based on the current study with Monte Carlo simulation code, it is shown that in a certain concentration, GNPs with higher dimensions contribute more dose to the tumor volume; while in a uniform distribution of GNP causes a remarkable increase in the absorbed dose. Also, it was observed that having a penetration margin for gold nanoparticles to healthy tissues can reduce the concentration of gold nanoparticles on the surface of tumor, resulting in reduction in the dose given to the tumor and larger sizes of gold nanoparticles showed an increase in the DEF, it also increases the DEF in lower energies. The use of gold nanoparticles in this study increased the optimal dose in tumor tissue.

When the GNP is large relative to the range of electrons generated therein, many low-energy electrons are trapped inside the GNP. Decreasing the size of the GNP, on the other hand, decreases the total number of photon interactions, leading to a reduced number of secondary electrons (Gadoue et al. 2017).

We encountered a number of uncertainties in this study: They are listed below.

- The Monte Carlo method is random in calculating doses.
- Lack of real mass density of tumor and different organs.
- Ignoring the real shape of the tumor and its characteristics.
- The purity percentage of gold nanoparticles is not considered
- Not taking into account how the nanoparticles are injected and precise entry into adjacent organs along the crossing path.
- The lack of an exact equation for the distribution of nanoparticles on the tumor.
- Using ideal mathematical models that can make a difference in the real situation.

In this investigation, the source has been assumed as a point which is different from the clinical case. And it could be considered as one of the limitations of this work.

Given the fact that therapeutic applications of GNPs in acquiring the proper dose enhancement have demanded much attention in recent years, defining the proper size and plan of GNP distribution on the tumor area would be considered extremely vital for pre-treatment plans.

Also, macroscale and nanoscale simulation is not enough for the correct consideration of the radiosensitizing effect at the cellular level. But this study can be one of the reasons for increasing the dose and the sensitivity.

5. Conclusion

Gold nanoparticles due to their high atomic number (Z) provide remarkable photoelectric cross-section and lead to enhancement of absorbed radiation dose in a tumor. This is due to a wide ranges of electrons emanated from photoelectric reactions inside and in the vicinity of the tumor. Since the cross-section of the photoelectric reaction falls rapidly at higher photon energies, the effect of dose enhancement vanishes at megavoltage energy range.

The collision of the photons with gold nanoparticles causes significant photoelectric interaction on the tumor, which produces secondary particles such as characteristic X-ray, photoelectrons and Auger electrons and they increase the dose as well (Gonzalez and Higgins 2017).

In this work, with 18 mgAu/ml homogeneous GNPs in 50, 95 and 250 keV photon energy for the case of a tumor located at 2 cm depth, DEF is 3.08, 2.41 and 1.22 respectively, In other words, the observations and results confirmed that gold nanoparticles can increase the dose of the tumor during radiotherapy.

Acknowledgments

The authors would like to thank Mr. Mahdi Ghorbani, Professor of Medical Physics, Shahid Beheshti University of Tehran, Iran for his helful consultation in the preparation of this manuscript.

References

- Adam JF, Biston MC, Rousseau J, Boudou C, Charvet AM, Balosso J, Estève F, Elleaume H (2008) Heavy element enhanced synchrotron stereotactic radiotherapy as a promising brain tumour treatment. Physica Medica 24: 92–97. https://doi.org/10.1016/j.ejmp.2008.02.003
- Alkilany AM, Murphy CJ (2010) Toxicity and cellular uptake of gold nanoparticles: What we have learned so far? Journal of Nanoparticle Research 12: 2313–2333. https://doi.org/10.1007/s11051-010-9911-8
- Balakin BV, Zhdaneev OV, Kosinska A, Kutsenko KV (2019) Direct absorption solar collector with magnetic nanofluid: CFD model and parametric analysis. Renewable Energy 136: 23–32. https://doi.org/10.1016/j.renene.2018.12.095
- Briesmeister JF (2000) MCNP-A general Monte Carlo N-particle transport code. Version 4C, LA-13709-M, Los Alamos National Laboratory.
- Brun E, Sanche L, Sicard-Roselli C (2009) Parameters governing gold nanoparticle X-ray radiosensitization of DNA in solution. Colloids and Surfaces B: Biointerfaces 72: 128–134. https://doi.org/10.1016/j.colsurfb.2009.03.025
- Chang M-Y, Shiau A-L, Chen Y-H, Chang C-J, Chen HH-W, Wu C-L (2008) Increased apoptotic potential and dose-enhancing effect of gold nanoparticles in combination with single-dose clinical electron beams on tumor-bearing mice. Cancer Science 99: 1479–1484. https://doi.org/10.1111/j.1349-7006.2008.00827.x
- Cho SH (2005) Estimation of tumour dose enhancement due to gold nanoparticles during typical radiation treatments: A preliminary Monte Carlo study. Physics in Medicine and Biology 50: e15. https://doi.org/10.1088/0031-9155/50/15/N01
- Cho WS, Cho M, Jeong J, Choi M, Han BS, Shin HS, Hong J, Chung BH, Jeong J, Cho MH (2010) Size-dependent tissue kinetics of PEG-coated gold nanoparticles. Toxicology and Applied Pharmacology 245: 116–123. https://doi.org/10.1016/j.taap.2010.02.013
- Gadoue SM, Toomeh D, Zygmanski P, Sajo E (2017) Angular dose anisotropy around gold nanoparticles exposed to X-rays. Nanomedicine: Nanotechnology, Biology, and Medicine 13: 1653–1661. https://doi.org/10.1016/j.nano.2017.02.017
- Gonzalez MT, Higgins MM (2017) Influence of Gold Particle Concentration and X-Ray Energy in Radiosensitization. Transactions 117: 33–35.
- Granqvist CG, Buhrman RA, Wyns J, Sievers AJ (1976) Far-infrared absorption in ultrafine Al Particles. Physical Review Letters 37: 625–629. https://doi.org/10.1103/PhysRevLett.37.625
- Griffiths HJ (1989) Tissue Substitutes in Radiation Dosimetry and Measurement. No. 4 . Radiology 173: 202–202. https://doi.org/10.1148/radiology.173.1.202
- Guo A, Fu Y, Wang G, Wang X (2017) Diameter effect of gold nanoparticles on photothermal conversion for solar steam generation. RSC Advances 7: 4815–4824. https://doi.org/10.1039/C6RA26979F
- Hainfeld JF, Dilmanian FA, Slatkin DN, Smilowitz HM (2008) Radiotherapy enhancement with gold nanoparticles. Journal of Pharmacy and Pharmacology 60: 977–985. https://doi.org/10.1211/jpp.60.8.0005
- Hainfeld JF, Slatkin DN, Smilowitz HM (2004) The use of gold nanoparticles to enhance radiotherapy in mice. Physics in Medicine and Biology 49. https://doi.org/10.1088/0031-9155/49/18/N03
- Hayashi C, Uyeda R, Tasaki A (1997) Ultra-fine particles: exploratory science and technology, Translation of the Japan report of the related ERATO Project 1997: 193–195.
- Herold DM, Das IJ, Stobbe CC, Iyer RV, Chapman JD (2000) Gold microspheres: A selective technique for producing biologically effective dose enhancement. International Journal of Radiation Biology 76: 1357–1364. https://doi.org/10.1080/09553000050151637
- Kobayashi K, Usami N, Sasaki I, Frohlich H, Le Sech C (2003) Study of Auger effect in DNA when bound to molecules containing platinum. A possible application to hadrontherapy. In: Nuclear Instruments and Methods in Physics Research, Section B: Beam Interactions with Materials and Atoms 199: 348–355. https://doi.org/10.1016/S0168-583X(02)01532-X
- Lin Y, McMahon SJ, Scarpelli M, Paganetti H, Schuemann J (2014) Comparing gold nano-particle enhanced radiotherapy with protons, megavoltage photons and kilovoltage photons: A Monte Carlo simulation. Physics in Medicine and Biology 59: 7675–7689. https://doi.org/10.1088/0031-9155/59/24/7675
- Mello RS, Callisen H, Winter J, Kagan AR, Norman A (1983) Radiation dose enhancement in tumors with iodine. Medical Physics 10: 75–78. https://doi.org/10.1118/1.595378
- Mesbahi A, Jamali F, Gharehaghaji N (2013) Effect of photon beam energy, gold nanoparticle size and concentration on the dose enhancement in radiation therapy. BioImpacts 3: 29–35. https://doi.org/10.5681/bi.2013.002
- Mousavie Anijdan S, Shirazi A, Mahdavi S, Ezzati A, Mofid B, Khoei S, Zarrinfard M, Rabi Mahdavi S (2012) 10 J. Radiat. Res Megavoltage dose enhancement of gold nanoparticles for different geometric set-ups: Measurements and Monte Carlo simulation.
- Prezado Y, Fois G, Le Duc G, Bravin A (2009) Gadolinium dose enhancement studies in microbeam radiation therapy. Medical Physics 36: 3568–3574. https://doi.org/10.1118/1.3166186
- Rahman WN, Bishara N, Ackerly T, He CF, Jackson P, Wong C, Davidson R, Geso M (2009) Enhancement of radiation effects by gold nanoparticles for superficial radiation therapy. Nanomedicine: Nanotechnology, Biology, and Medicine 5: 136–142. https://doi.org/10.1016/j.nano.2009.01.014
- Ranjbar H, Shamsaei M, Ghasemi MR (2010) Investigation of the dose enhancement factor of high intensity low mono-energetic X-ray radiation with labeled tissues by gold nanoparticles. Nukleonika 55(3): 307–312.

- Robar JL, Riccio SA, Martin MA (2002) Tumour dose enhancement using modified megavoltage photon beams and contrast media. Physics in Medicine and Biology 47: 2433–2449. https://doi.org/10.1088/0031-9155/47/14/305
- Roeske JC, Nuñez L, Hoggarth M, Labay E, Weichselbaum RR (2007) Characterization of the Theorectical Radiation Dose Enhancement from Nanoparticles. Technology in Cancer Research & Treatment 6: 395–401. https://doi.org/10.1177/153303460700600504
- Sakata D, Kyriakou I, Okada S, Tran HN, Lampe N, Guatelli S, Bordage M-C, Ivanchenko V, Murakami K, Sasaki T, Emfietzoglou D, Incerti S (2018) Geant4-DNA track-structure simulations for gold nanoparticles: The importance of electron discrete models in nanometer volumes. Medical Physics 45: 2230–2242. https://doi.org/10.1002/mp.12827
- Sheikh-Bagheri D, Rogers DWO (2002) Monte Carlo calculation of nine megavoltage photon beam spectra using the BEAM code. Medical Physics 29: 391–402. https://doi.org/10.1118/1.1445413
- Sung W, Schuemann J (2018) Energy optimization in gold nanoparticle enhanced radiation therapy. Physics in Medicine and Biology 63: e13. https://doi.org/10.1088/1361-6560/aacab6
- Sung W, Ye SJ, McNamara AL, McMahon SJ, Hainfeld J, Shin J, Smilowitz HM, Paganetti H, Schuemann J (2017) Dependence of gold nanoparticle radiosensitization on cell geometry. Nanoscale 9: 5843–5853. https://doi.org/10.1039/c7nr01024a
- Zhang SX, Gao J, Buchholz TA, Wang Z, Salehpour MR, Drezek RA, Yu TK (2009) Quantifying tumor-selective radiation dose enhancements using gold nanoparticles: A monte carlo simulation study. Biomedical Microdevices 11: 925–933. https://doi.org/10.1007/s10544-009-9309-5
- Zheng Y, Hunting DJ, Ayotte P, Sanche L (2008) Radiosensitization of DNA by Gold Nanoparticles Irradiated with High-Energy Electrons. Radiation Research 169: 19–27. https://doi.org/10.1667/rr1080.1